EXPERIMENTAL MEASUREMENT OF ON-VEHICLE ROLLING TIRE CONTACT PATCH SHEAR ENERGY INTENSITY AT VARIOUS SLIP ANGLES

by

Nagarjun Chandrashekar

A thesis submitted to the faculty of
The University of North Carolina at Charlotte
in partial fulfillment of the requirements
for the degree of Master of Science in
Mechanical Engineering

Charlotte

2017

Approved by:

_____
Dr. Peter T. Tkacik

_____
Dr. Russell Keanini

_____
Dr. Saiful Bari

ABSTRACT

NAGARJUN CHANDRASHEKAR. Experimental measurement of on-vehicle rolling tire contact patch shear energy intensity at various slip angles (Under the direction of DR. PETER T. TKACIK)

It has long been accepted that tire wear is directly related to the energy generated due to shear at the contact patch. Tire wear at any given point on the contact patch is proportional to the amount of shear energy intensity acting at that point. In this research, shear energy intensity as a product of sliding displacements and frictional force at a sufficient number of points is mapped across the tire contact patch.

The phenomenon of Frustrated Total Internal Reflection (FTIR) [1] is used to measure the normal stress distribution across the contact patch. The normal stress is calculated based on the amount of light intensity acting at each pixel across the contact patch. The tread blocks on the tire are painted with white dots, and a similar method without the dimpled plastic of the FTIR is used to obtain the point by point tread block displacements. With the help of computer image processing, shear energy intensity as a function of frictional force and tread block displacements are mapped at multiple time stamps across the contact patch at various slip angles.

Results show that the total shear energy acting across the contact patch increase with increasing slip angles. This demonstrates that the tire is going to wear more aggressively as the slip angle increases. The shear energy intensity mapped across the contact patch show that the tire is going to experience more irregular wear as the slip angle increases. From the results, it is seen that the shear energy intensity is more uniformly spread out at very low slip angles and at higher slip angles, the shear energy intensity is almost zero at the leading edge

of the contact patch and maximum at the trailing edge of the contact patch. This corroborates the premise that highest shear is at the trailing edge of the contact patch.

DEDICATION

I dedicate this thesis research to my parents and my friends who have encouraged me throughout this journey.

I also dedicate this thesis research to my brother, Shayan Chandrashekar who has constantly supported and motivated me.

ACKNOWLEDGEMENTS

I would like to begin by thanking my advisor, Dr. Peter T. Tkacik for guiding me throughout the thesis research work. Dr. Tkacik's insights from his years of experience from the tire industry proved to be valuable for this research work.

I would like to thank Dr. Russell Keanini and Dr. Saiful Bari for their help and suggestions, and also for being on the committee for this research.

I would also like to thank a fellow student and colleague, Piyush Gulve for his support and commitment to this research work.

Special thanks to Tucker Bisel and Adit Miser for helping me with image processing for this research work.

A definite thank you to Mr. Kile Stinson for helping me in the experimental setup and providing insights on the design.

Some fellow students Kapil Gaur, and Surya Phani Krishna Nukala deserve acknowledgement for their assistance with research activities.

Lastly, I would like to thank the Mechanical Engineering Department for their professionalism, support, and encouragement to be involved with on campus projects pursuant with my own career interests.

TABLE OF CONTENTS

LIST OF FIGURES

LIST OF TABLES

CHAPTER 1: INTRODUCTION

1.1 Organization of Thesis

Chapter 1 provides the reader with a brief introduction to tire contact patch and the motivation behind this research work. The phenomenon of Frustrated Total Internal Reflection (FTIR) is explained, along with the Footprint Axis System, tire contact forces and stresses, tire geometry, slip angles, visco-elasticity, friction and shear energy intensity.

Chapter 2 describes the experimental setup used for this research work, along with the test procedure and the images obtained from the high-speed camera are shown.

Chapter 3 provides detailed discussions of results from the experiment, conclusions and future work of this research.

1.2 Motivation

Tire contact patch (footprint) is a part of the tire which is in actual contact with the road surface. The contact patch will vary in shape and size depending on the geometry of the tire and the suspension settings. Accurately measuring the tire footprint plays an important role in analyzing the interaction of the tire with the road surface. Tire footprint physics is fundamental to the generation of vehicle control forces, tire wear, and tire structural mechanics. Tires with a higher profile (aspect ratio) tend to have a long and narrow contact patch. The longer, narrower contact patch gives these tires a smooth ride and allows them to handle in a predictable manner. On the other hand, most high performance and ultra-high performance summer tires have low profile. Thus, the contact patch is shorter and wider, which gives them strong cornering stiffness and traction.

It is important to visualize deformation of tire tread, and study the effects of shear energy intensity as a function of tire wear. Thus, static footprint imaging is insufficient. Studying the pattern in which the contact patch changes by altering various vehicle suspension parameters is of prime importance and hence the dynamic imaging of a rolling tire contact patch is necessary.

Various methods have been previously tried and tested to capture the footprint and the load distribution of a rolling tire contact patch. Earlier attempts were made to find the load distribution across the contact patch by loading the tire onto clay or Plaster of Paris. The portion with the deepest impression was considered as the place where the maximum amount of pressure was acted upon. However, this method was not very accurate, as it is difficult to find a material with the right plasticity. Hence, any low-pressure area would simply deform along with the surrounding high pressure areas. One of the early attempts to use printing techniques was formulated by Morton [6], which was based on a device called a Kinetograph. It was basically a rubber mat with a flat upper surface and a rigged lower surface on which ink could be spread. When load was applied on the upper surface, the lower rigged surface would press against a sheet of paper, and a series of parallel lines were printed. The width of the line at any given point would give the pressure being applied at that point. [1]. Elftman [7], was one of the first persons to use a direct visualization technique. His apparatus consisted of a floodlit glass plate, which replaced ink and paper on the underside of the mat used by Morton [6]. The variation in pressure was found based on the proximity of the flattened ridges onto one another. But, this method was also not very accurate since it was fairly course and could not study the detailed behavior.

In the coming years, a device called pedobarograph was proposed by Chodera [8], which was used to capture the pressure distribution under people's feet. It was further refined by Betts and Duckworth [9]. Gentle [1] has adopted some of the concepts used, to construct an apparatus for the use with tires. This apparatus relies heavily on the phenomenon of Frustrated Total Internal Reflection (FTIR). His apparatus consisted of a tire, loaded by a dead weight and lever system, observed from below by a monochromatic video camera [1]. The output from the video camera was displayed onto a monitor. This technique was much more advanced compared to the ink and paper technique, and provided results with higher accuracy. However, these results are still insufficient, and cannot simulate the road conditions, as the tire was not mounted onto the vehicle. Apart from load, the vehicle suspension settings and wheel alignment play a major role in determining the pressure distribution across the contact patch. In this study, the concept of FTIR has been adopted and an actual car with various suspension settings has been used to simulate the footprint on road conditions and get accurate results. Along with the pressure distribution, the displacement vectors at multiple points across the tire contact patch have been calculated to map the shear energy intensity to predict how the tire is going to wear at various slip angles.

1.3 Frustrated Total Internal Reflection (FTIR)

When a light wave reaches a boundary between different materials with different refractive indices, the light wave in general will be partially refracted at the boundary surface, and partially reflected. However, if the angle of incidence is greater than the critical angle, then the light wave will not cross the boundary, but will be totally internally reflected back into the dense medium. However, there is still an electric disturbance in the low-density medium within a few wavelengths of the interface, even though all the light energy has been

reflected. If now a third medium is brought close to the interface, with a high optical density, then the light will be partially transmitted across the gap, and so the total internal reflection is frustrated [1].

Figure 1 shows how the phenomenon of frustrated total internal reflection is used in this experiment. Light from a high-powered LED is shown into a 19mm (¾") thick glass panel, at a certain angle so that total internal reflection occurs inside the glass panel. A dimpled cloth, stuck to the glass panel, is used as a third medium. At the point of contact, light escapes from the glass and illuminates the dimpled cloth. When observed from below, a bright green color illuminated at the point of contact can be seen. If the pressure at the point of contact is high, then the brightness of the green patch increases. As a result, the load distribution as a function of light intensity across the contact patch can be determined.

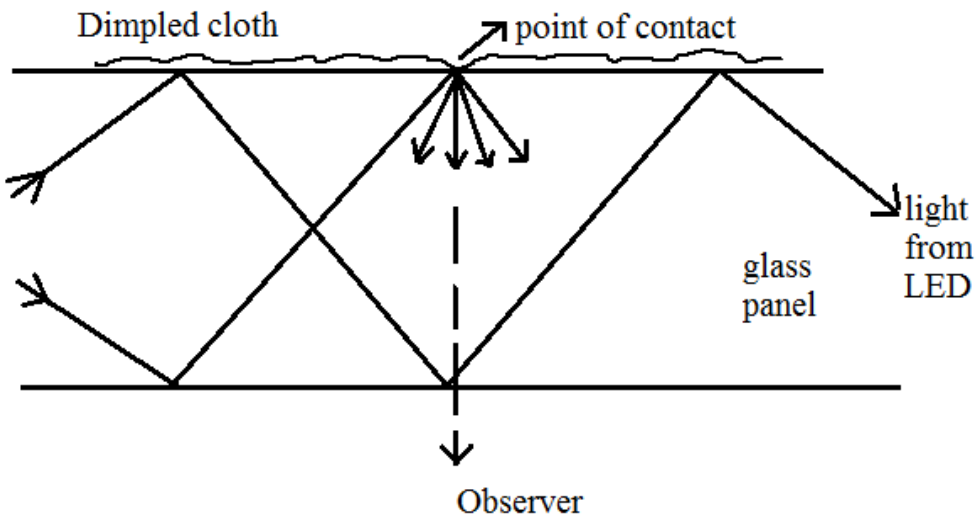

Figure 1.1: Working principle of frustrated total internal reflection [1].

1.4 Tire footprint or contact patch

Tire footprint or contact patch is a portion of the tire which comes in contact. as the tire rolls across the road surface. It is most commonly used in pneumatic tires, where air is used to pressurize the tire. Generally, the three main characteristics used for describing a rolling elastic tire are [10],

a. The area of contact between the tire and the road.

b. The slip or relative motion between the tire and the road.

c. Normal and tangential contact stresses between the tire and the road.

Tire footprint mechanics or physics involves footprint geometry, tread pattern geometry, contact stresses, and the sliding displacements. Since the forces needed for vehicle support, guidance and maneuvers all arise in the tire contact area, study of these characteristics and application of the resulting theory should improve both the mechanical properties of the tire and the control of vehicles [10].

In this section, the footprint axis system is described, along with the contact stresses and the sliding displacements.

1.4.1 The footprint axis system (FAS)

The tire footprint is described here in terms of an axis system based on, but not identical to the SAE Tire Axis System [2]. The Footprint Axis System (FAS) establishes a viewpoint and provides a coherent description of tire footprint behavior [4]. The differences between the SAE Tire Axis System and the Footprint Axis System arise due to the fact that the instrumentation used for the measurement of the tire footprint behavior uses the road surface as the fixed orientation, whereas the instrumentation used to measure the gross tire

forces and moments has a wheel based orientation. Hence, it is better to describe the footprint behavior, where the road surface is considered as the fixed orientation.

The Footprint Axis system (FAS) as shown in figure 2 is a three-axis orthogonal Cartesian coordinate system, which has its origin at the contact center of the road plane. The road plane is a plane which is tangential to the road surface and the contact center is a point in the road plane where the line defined by the wheel plane (the plane halfway between the wheel flanges) to road plane intersection is cut by the projection of the spin axis onto the road plane [3]. Hence, the contact center is defined by the wheel instead of the tire, and it is a common point for the FAS and the SAE Tire Axis System.

The X-axis in the FAS is on the road plane and corresponds to the direction of the tire's trajectory velocity. The Y-axis in the FAS is also on the road plane, and is perpendicular to the X-axis. The Y-axis is positive, if it is moving towards the right side of the road plane, and it is negative if its moving towards the left of the road plane. The Z-axis of the FAS is a cross product of the positive X and the positive Y axis and is pointing downwards into the road plane.

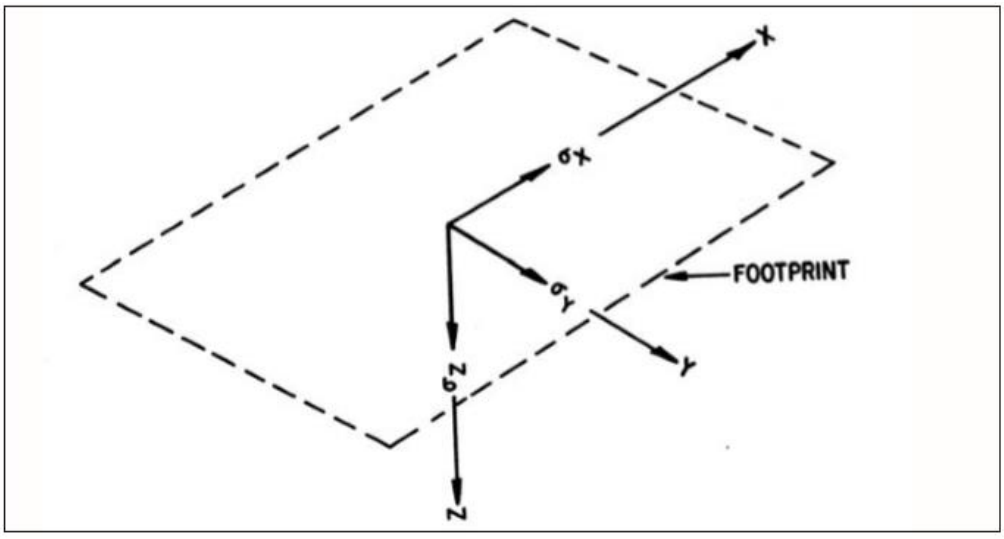

Figure 1.2: Footprint Axis System [5]

1.4.2 Tire contact forces and stresses

Stress analysis is a branch of mechanics which is concerned with the quantitative determination of internal stresses and strains produced in a body as the result of externally applied loads and deformation [10]. It is both theoretical and experimental. The stress analysis of a tire should provide the magnitude, direction as well as the type of stress acting on the tire under each loading condition.

Figure 1.2 shows the three types of stresses acting on the tire, when the tire is in contact with the road surface. The direction of the stresses acting on the contact patch, as shown in figure are considered to be positive. The stress in the X-axis has both positive and negative values. Stress in the positive direction implies that the tire is being pushed forward, and similarly, stress in the negative direction implies that the tire is being pushed rearward. The stress in the Y-axis also has both positive and negative values. Stress in the positive direction implies the tire is being pushed to the right, and similarly, stress in the negative direction implies the tire is pushed towards the left. Stress in the Z-axis supports the tire, basically keeps it from sinking into the ground. Thus, there are only negative values.

The forces, both normal and shear, and slip motions in the contact patch are important because they affect the tire's resistance to wear [3]. Tire wear can occur in different forms, which are regular wear (long term wear), and irregular wear. Regular wear is a type of tire wear which occurs uniformly over a long period of time. On the other hand, irregular wear has many forms, such as shoulder wear (due to excessive camber), heel-toe wear (due to faulty suspension), and so on. All of these wear types are related to the combination of normal and shear force, and the amount of slip that occurs as tread elements pass through the contact patch [3]. Even when the tire is rolling forward and not generating lateral forces,

shear force is generated across the contact patch. Theoretically, a radial tire will roll forward for a distance which is equal to the belt package. But, since the actual circumference of the tire is more than the belt package (due to the thickness of the tread pattern), the tire must accommodate for the difference in the distance when rolled forward. Typically, the fore-and-aft component of the shear force grows uniformly from zero at the leading edge of contact, reaching a maximum towards the trailing edge. At this point in time, the tread block elements are released from the road surface and recovers their unloaded shapes. This buildup and release of the shear displacement at the contact patch is the cause of the difference between the tire circumference and the distance travelled in one revolution. During heavy braking, cornering, and acceleration, the slip patterns are more severe and complex. Hence, the study of these slip patterns is important to predict the tire wear and tire behavior.

1.4.3 Footprint Geometry

Figure 1.3 (a) shows the image of a tire footprint, rolling in the upward direction. The X and Y coordinates have been marked in the figure (b). The edge of the footprint with the most positive X value is called as the leading edge, and the edge of the footprint with the most negative X value is called as the trailing edge of the footprint. Tire tread blocks are the elements which are generated by the grooves cutting across the central rib. The first edge of the tread block to come in contact with the road surface is called as heel (leading edge of the tread block), and the last edge of the tread block to come in contact with the road surface is called as toe (trailing edge of the tread block). It is important to note that the leading edge and trailing edge of the footprint and the tire tread block elements are reversed.

Generally, there are two displacements to be considered in a contact patch. U velocity corresponding to the X direction, and V velocity corresponding to the Y direction as per the figure.

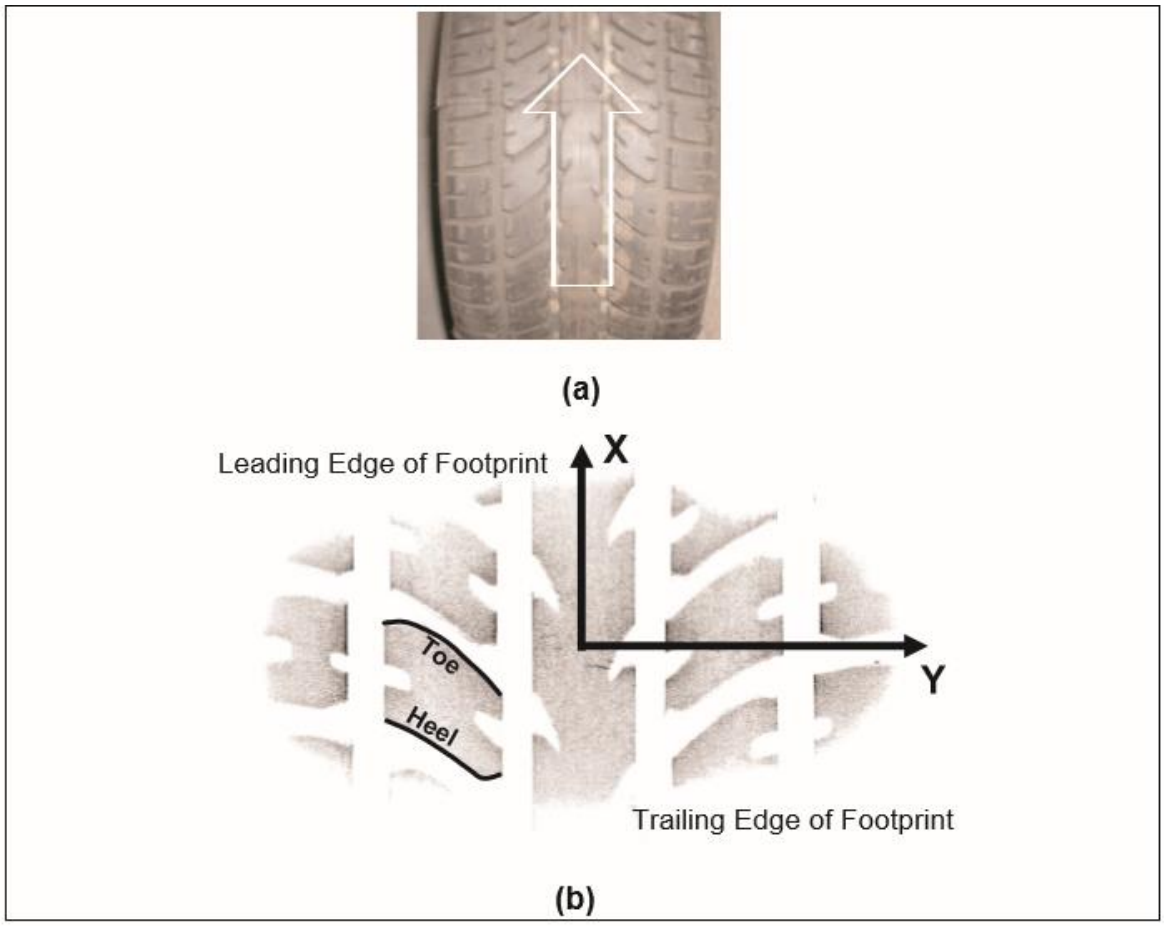

Figure 1.3: Tire footprint geometry [3].

1.5 Slip angle

From the vehicle dynamics point of view, slip is considered to be relative motion between the tire and the surface it is rolling on. Slip can be generated in two ways, one is when the tire's rotational speed is greater or lesser compared to the free rolling speed (longitudinal slip) and the other is when there is an angle between the rolling tire's actual direction of travel and the direction towards which it is pointing (lateral slip). This angle is

called as slip angle. Slip angle is created when a rolling tire is subjected to lateral force. As a result, the tire tends to drift sideways. This can be illustrated in Figure 1.4 [13].

The tread block elements come in contact with the road surface as the tire rolls forward, and will remain in their normal position. Thus, no lateral force is generated. But as the tire advances further at the angle of its direction of travel, the tread elements remain in the position of their original contact with the road and are therefore deflected sideways with respect to the tire [13]. As a result, the lateral force builds up and the tread block elements move towards the trailing edge of the contact patch, up to a point where the tread block elements overcome the friction and slip occurs. This is clearly illustrated in figure 1.4 [13].

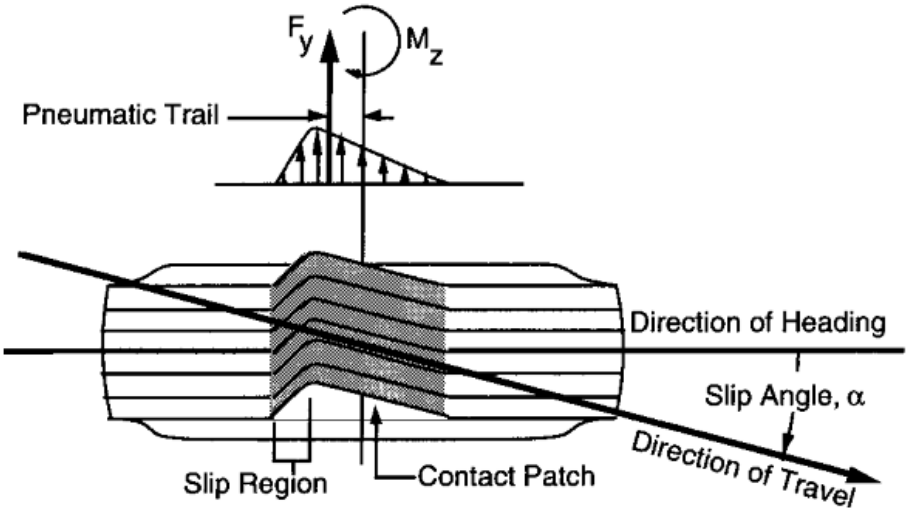

Figure 1.4: Rolling tire deformation under a lateral force [13].

1.6 Visco-elasticity

Visco-elasticity is the property of certain materials, which exhibit both viscous and elastic characteristics when undergoing deformation. Viscous materials are substances which have high viscosity and resist flow over a period of time when stress is applied. Elastic materials on the other hand are materials which store energy when deformed and then return

back to its original state once the stress is removed. Purely elastic materials do not dissipate energy when load is applied and removed. However, a visco-elastic material loses energy when a load is applied. This energy loss is called as hysteresis loss.

1.6.1 The loss tangent (Tan(δ))

The premier polymeric friction parameter is the loss tangent, (Tan(δ)) [14]. This parameter is found by cyclically loading the polymer samples and recording the deformation. Due to the hysteresis losses, there will be a phase lag between the stress and the strain (as shown in figure 1.5). Modulus is defined as the ratio of stress to strain, and for polymers, it is referred to as the complex modulus E^*.

$$E^* = E' + iE'' \text{ [14].}$$

Where, E' is referred to as the real modulus (a component of strain in the direction of stress) and E" is the loss modulus (out of phase stress over strain). The ratio of loss modulus over real modulus (E"/E') gives the Tangent of an angle delta (phase angle by which the strain lags behind the applied stress). It is useful due to its correlation to the friction coefficient.

$$\text{Tan}(\delta) = \frac{E''}{E'} \text{ [14]}$$

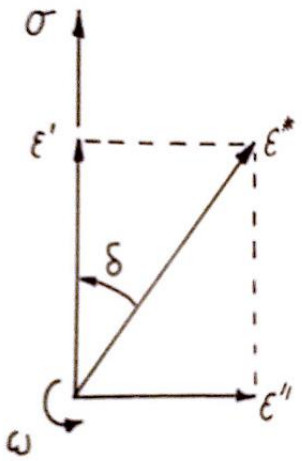

Figure 1.5: Phase lag between stress and strain (Tan(δ)) [14].

1.7 Friction with polymers

The two main sources of friction with polymers are friction due to adhesion and deformation. Friction caused by deformation occurs as a mechanical interlocking of the polymer and a coarse surface [14]. The mechanical interlocking increases as load increases, and results in a friction coefficient proportional to the contact stresses. On the other hand, no slip occurs for friction due to adhesion. What occurs is the release of the contact area and a slight relative shift of the contact area. The released zone on a polymer travels across the contact zone and is called as 'Shallamach waves'.

As a glass panel, which has a smooth surface was used in this study, the friction was considered to be adhesive, and the experimental results of Tkacik [14] demonstrated that the coefficient of friction is a function of normal stress, G', and the loss tangent. It is given by the equation,

$$\frac{0.262200\ G'Tan(\delta)}{(\sigma)^{0.826097}} = \mu \text{ [14]}$$

Where, G' is the real shear modulus.

1.8 Shear energy intensity

It has long been demonstrated that energy generated due to shear stress at the tire contact patch is directly related to tire wear. In order to calculate shear energy, it is necessary to calculate the shear stress and the displacements at sufficient number of points across the contact patch.

Shear energy intensity is the total energy crossing the boundary between the tire and the road, arising from shear stresses and displacements at the interface, and reported on a

per-unit area basis [3]. For every pass-through contact, the path integral from the below equation can be calculated at each location in the tread pattern, where a point on the tire tread is located.

The shear energy intensity or work done is given by [3],

$$W_{ij} = \oint_S \overline{F_{ij}} \bullet d\overline{S}_{ij}$$

Where,

W_{ij} = shear work at point ij.

F_{ij} = Footprint force vector at point ij, on the tread surface as a function of S.

i = Lateral position index with respect to tread surface.

j = Circumferential position index with respect to tread surface.

dS_{ij} = Differential footprint displacement vector.

S = Path of integration. Physically, the path of motion of a point ij on the tread relative to a fixed point on the road surface during contact.

CHAPTER 2: METHODOLOGY

2.1: Experimental setup

The experimental setup, as developed by Gulve [15], consists of a Porsche 911 Carrera, fitted with 205/50ZR17 tires at the front and 255/40ZR17 tires on the rear, sitting on a specially modified four-post lift, as shown in figure 2.1. The tire pressure on the Porsche was set to the OEM rated pressure. The height at which the four-post lift sits on the ground has been slightly adjusted, to make sure the lift is perfectly leveled. The guideway on the four-post lift has been given two precision cut-outs over which a 559mm x 407mm x 19mm thick glass panel at the front end (shown in figure 2.2), and a 407mm x 407mm x 19mm thick glass panel at the rear end (shown in figure 2.3), mounted to a rubber frame sits. A frame has been built to mount a pair of single high-powered LED lights on either side of the glass panel. The height and angle at which the LEDs are mounted are adjusted accordingly, to achieve total internal reflection inside the glass panel, as shown in figure 2.4.

As a lot of lateral load will be applied while carrying out the test, lateral rubber bumpers have been mounted on either side of the LED lights to hold the glass panel in place. A thin dimpled plastic sheet has been pasted to a thin plastic frame and is placed on top of the glass panel to achieve frustrated total internal reflection (as shown in figure 2.5). Hunter wheel alignment machine, along with DSP700 wheel alignment heads (figure 2.6 and figure 2.7) are used to continuously monitor and measure the suspension settings such as, camber, and toe, while the test is being performed. A high-speed video camera is placed below the glass panel and is set at multi-point focus, to capture the entire rolling tire contact patch

without losing resolution. This high- speed video camera can capture up to 60 frames per second at 3840 pixels of 4K Ultra High Definition resolution.

The tread pattern of the front tire, which rolls over the glass panel has been painted with white dots (shown in figure 2.8), in order to get the point by point tread block deformation on the contact patch, as the tire rolls across the glass panel.

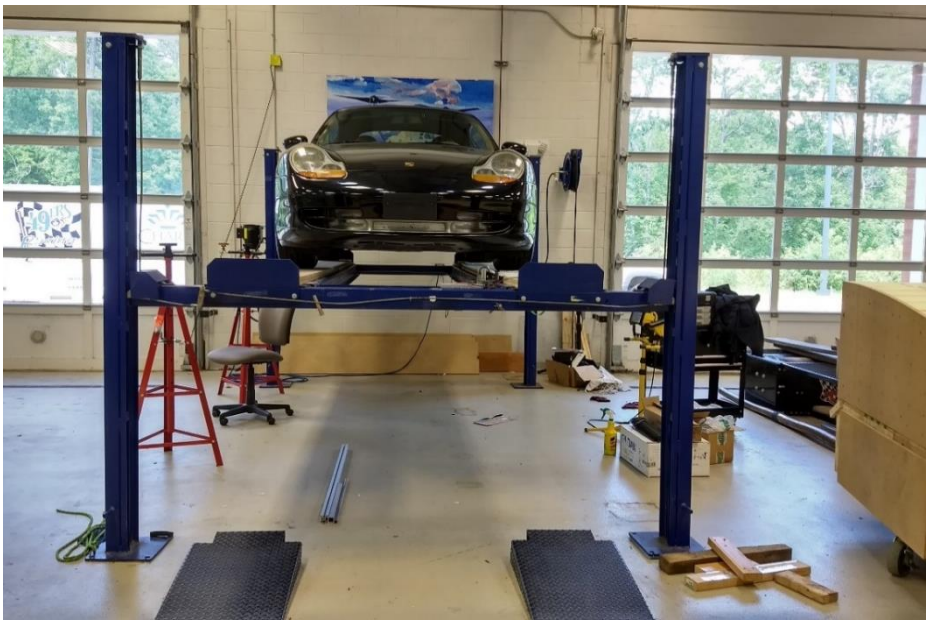

Figure 2.1: Porsche 911 sitting on the modified four-post lift.

Figure 2.2: 559mm x 407mm x 19mm thick glass panel mounted onto a rubber frame.

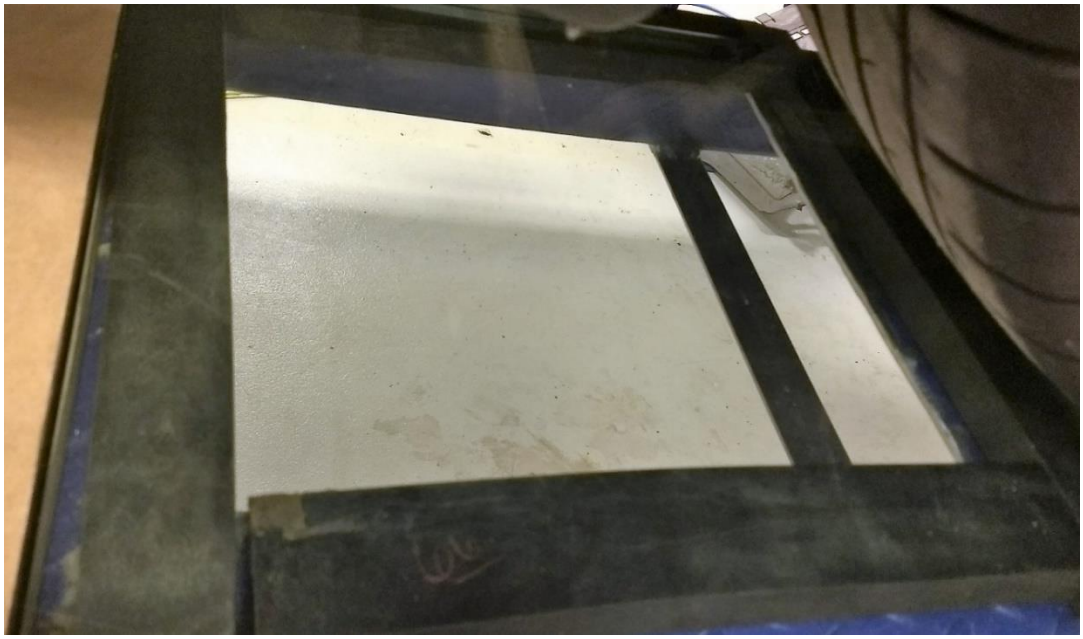

Figure 2.3: 407mm x 407mm x 19mm thick glass panel mounted on rubber frame.

Figure 2.4: High powered LED lights mounted onto a frame to achieve FTIR.

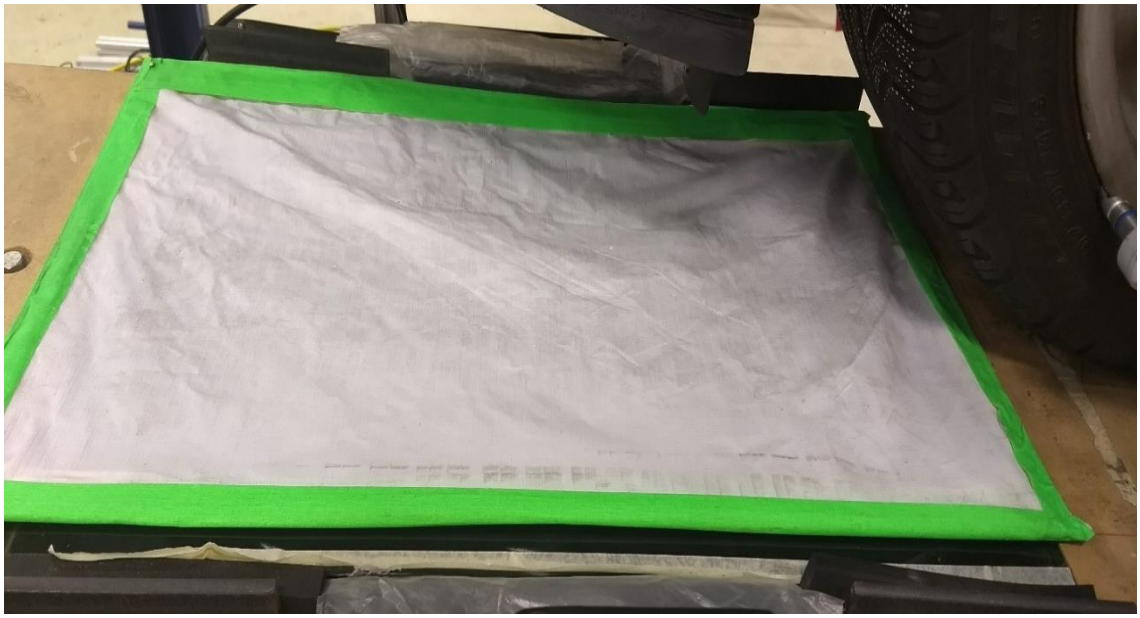

Figure 2.5: Dimpled plastic sheet to achieve FTIR.

Figure 2.6: Hunter pro align wheel alignment system [12].

Figure 2.7: DSP700 wheel alignment (high speed wireless DSP) sensor [11].

Figure 2.8: Tread pattern of the tire painted with white dots.

2.2: Test Procedure

The alignment heads are mounted onto all the four tires and an initial caster sweep is done to get the wheel alignment readings. The standard OEM specified toe reading had to be changed to get zero degree of slip angle for the initial reading. The car was lifted using jack stands, and bearing plates were placed beneath the wheels to change the suspension settings such as toe. Slip angle is varied by adjusting the toe links of the vehicle suspension such that the two tires on an axle generate equal and opposite lateral forces. On the vehicle used for this experiment, toe linkages allow this angle adjustment up to 12 degrees total or 6 degrees of slip for the tire being measured. Once the toe was set to a specific value, the car was lifted back onto the jack stands to remove the bearing plates and the car is put back on the four-post lift. The wheel alignment readings are recorded and monitored continuously, as the car is rolled across the four-post lift. Each time the car was pushed back and forth, the steering wheel of the car was locked, just to make sure that the car does not sway from its path and roll over from the four-post lift. The front portion of the car was completely covered by a black cloth, to make sure that no external light falls on the glass panel.

Images of the contact patch of the tire, as it is rolled across the glass panel, are captured by the high-speed video camera. The high-speed video camera is mounted on a special type of jack stand to adjust the height in order to achieve the perfect resolution. Measurements are taken at each degree of slip angle. For each degree of slip angle, two measurements were taken (one with the dimpled plastic and one without). Images gathered with the dimpled plastic sheet placed on the glass panel are used to calculate the load distribution across the contact patch and the images obtained without using the dimpled plastic sheet are used to calculate the point by point tread block displacements. Shear energy

intensity across the contact patch is mapped using both the displacement data and the load data. The slip angles which were evaluated are mentioned in the Table 2.1. At low slip angles, the vehicle could be pushed back and forth manually, but at higher slip angles, the vehicle drag forces rise high enough that a cable winch system was developed to pull the vehicle across the glass.

Total toe (degrees)	Slip angle (degrees)	Slip angles evaluated (degrees)
0	0	
-2	1	1
-4	2	2
-6	3	3
-8	4	4
-10	5	5
-12	6	6

Table 2.1: List of slip angles at which shear energy intensity is measured.

The following figures show the normal load images using the FTIR technique gathered from the high-speed video camera at various slip angles, and also the greyscale displacement images using white tread dots on bare glass at various slip angles.

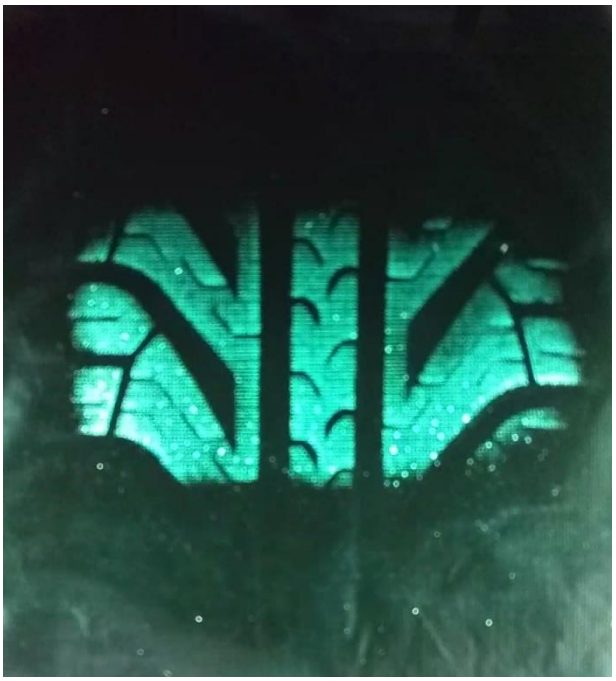

Figure 2.9: Normal load image using FTIR technique at 0^0 of slip angle.

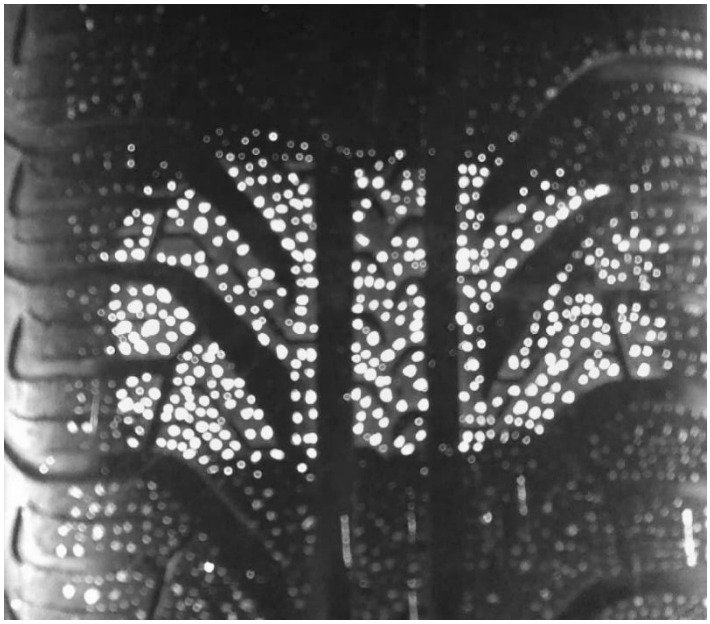

Figure 2.10: Greyscale displacement image using white tread dots on bare glass at 0^0 of slip angle.

Figure 2.11: Normal load image using FTIR technique at 1^0 of slip angle.

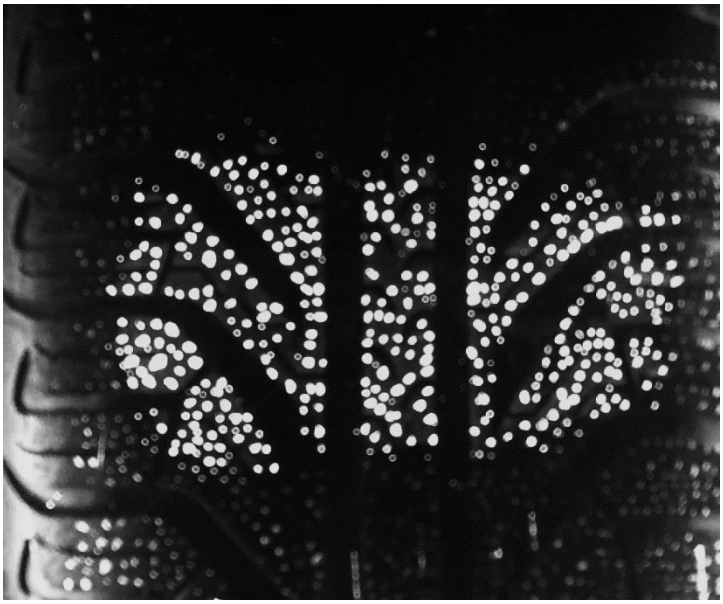

Figure 2.12: Greyscale displacement image using white tread dots on bare glass at 1^0 of slip angle.

Figure 2.13: Normal load image using FTIR technique at 2^0 of slip angle.

Figure 2.14: Greyscale displacement image using white tread dots on bare glass at 2^0 of slip angle.

Figure 2.15: Normal load image using FTIR technique at 3^0 of slip angle.

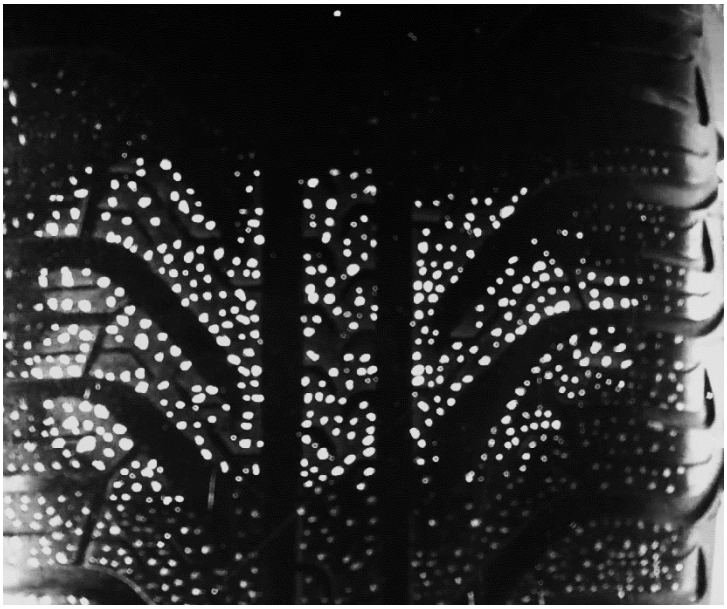

Figure 2.16: Greyscale displacement image using white tread dots on bare glass at 3^0 of slip angle.

Figure 2.17: Normal load image using FTIR technique at 4^0 of slip angle.

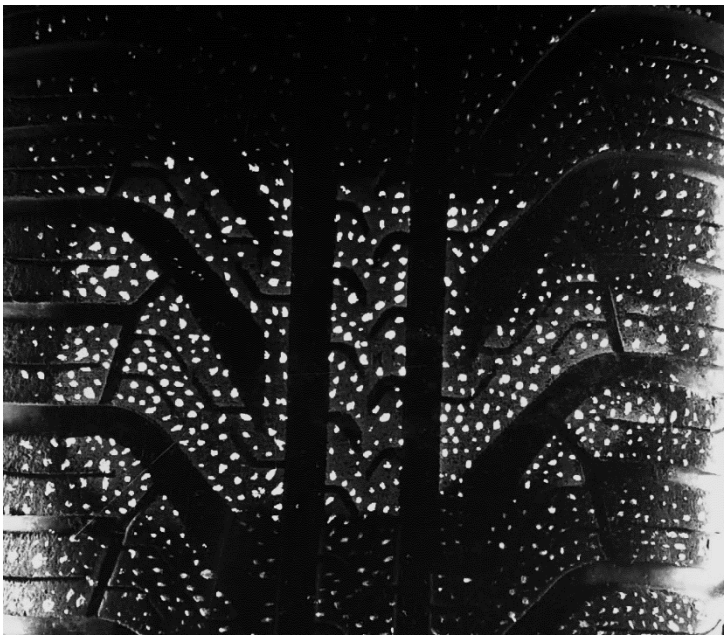

Figure 2.18: Greyscale displacement image using white tread dots on bare glass at 4^0 of slip angle.

Figure 2.19: Normal load image using FTIR technique at 5^0 of slip angle.

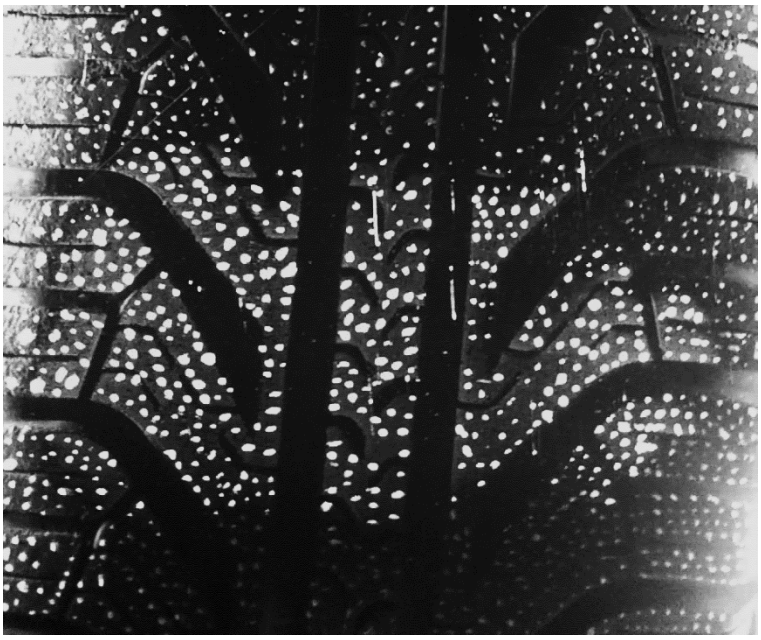

Figure 2.20: Greyscale displacement image using white tread dots on bare glass at 5^0 of slip angle.

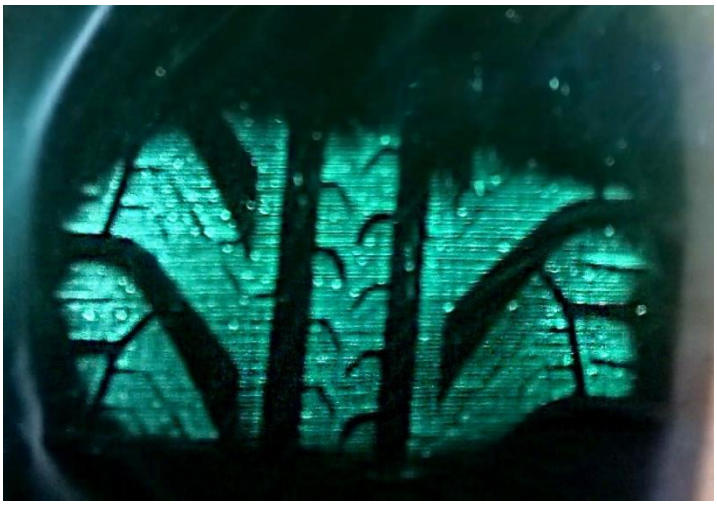

Figure 2.21: Normal load image using FTIR technique at 6^0 of slip angle.

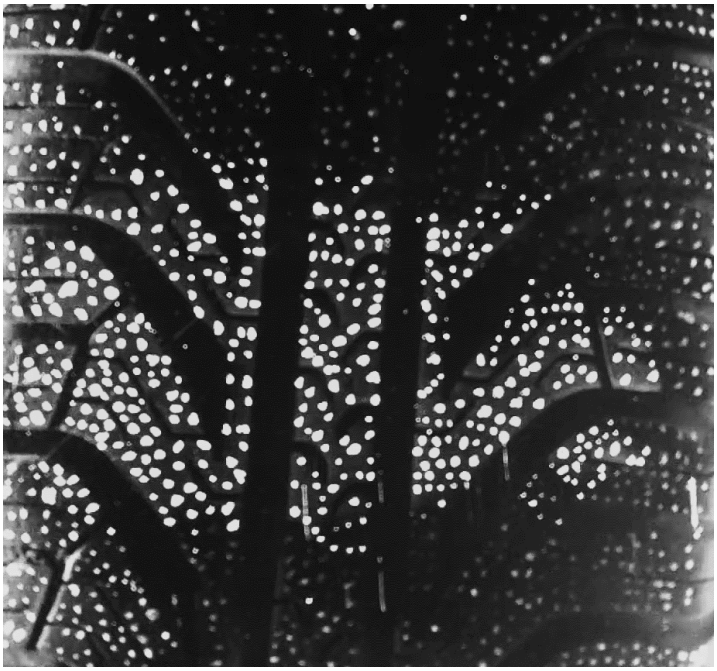

Figure 2.22: Greyscale displacement image using white tread dots on bare glass at 6^0 of slip angle.

CHAPTER 3: RESULTS AND CONCLUSION

3.1: Results and discussion

Several different computer image processing techniques have been used to calculate the shear energy intensity across the contact patch. Dynamic Studio, a software used for computer image processing is used for calculating the point-by-point tread block displacement vectors across the contact patch. As seen from the images below, dynamic studio captures a lot of random displacement vectors along with the actual data. This random data was later filtered out by using Matlab, which can also be used for computer image processing. Matlab is used for calculating the load distribution based on light intensity by using the images obtained from Frustrated Total Internal Reflection. From this method, the load acting on each pixel (N/pixel) is calculated and mapped across the contact patch.

Using the normal load, the normal stress is calculated for each pixel using the formula,

$$\sigma_n = \frac{\text{Normal force per pixel}}{\text{Area per pixel}} \qquad (N/m^2)$$

The area of each pixel was found to be $2\mu m^2$.

The values of Tan(δ) and G' were found to be 0.42 and 2.7 (N/m^2).

The values of Tan(δ), G' and the normal stress are substituted in the below equation to find the coefficient of friction for adhesion.

$$\frac{0.262200\ G'Tan(\delta)}{(\sigma)^{0.826097}} = \mu_{\text{adhesion}}\ [14]$$

From the coefficient of friction, the frictional force per pixel is calculated by multiplying normal force and coefficient of friction.

$$F_F = \mu_{\text{adhesion}} * \text{Normal force}$$

The frictional force calculated per pixel is then multiplied by the magnitude of the displacement vectors to find the shear energy intensity (work done) for each pixel. The shear energy intensity is then mapped across the contact patch by plotting contour plots in Matlab.

This procedure is repeated and the shear energy intensity is mapped across the contact patch for six different time stamps and the average total shear energy is calculated. The slip angle of the tire is then changed by increasing the toe and the entire procedure is repeated and the total average total shear energy across the contact patch is calculated for the new slip angle. Slip angles are changed from 0 degree to 1,2,3,4,5 and 6 degrees and the average total shear energy is calculated for 1,2,3,4,5 and 6 degrees of slip angle. The results are then plotted in an excel sheet. From the average total shear energy versus slip angle plot, it is demonstrated that the total shear energy increases with increase in slip angle. This implies that the tire is going to wear much faster, and also aggressively at higher slip angles. Also, from the shear energy intensity contour plots, it can be observed that the shear energy intensity is more uniformly spread out at very low slip angles. But, as the slip angle increases, the shear energy intensity is concentrated more at the trailing edge of the tire and is very less (almost close to zero) at the leading edge of the tire. This is due to the fact that maximum amount of slip occurs at the trailing edge of the tire at higher slip angles. This shows that the tire is going to have uneven or irregular wear at higher slip angles. By calculating the total

shear energy at different time stamps for each degree of slip angle, it is seen that the values are within an acceptable range. The experiment can be validated from these plots, as the shear energy across the contact patch is going to be similar at the same suspension settings. From this research, it can be seen how the tire is going to wear at different slip angles.

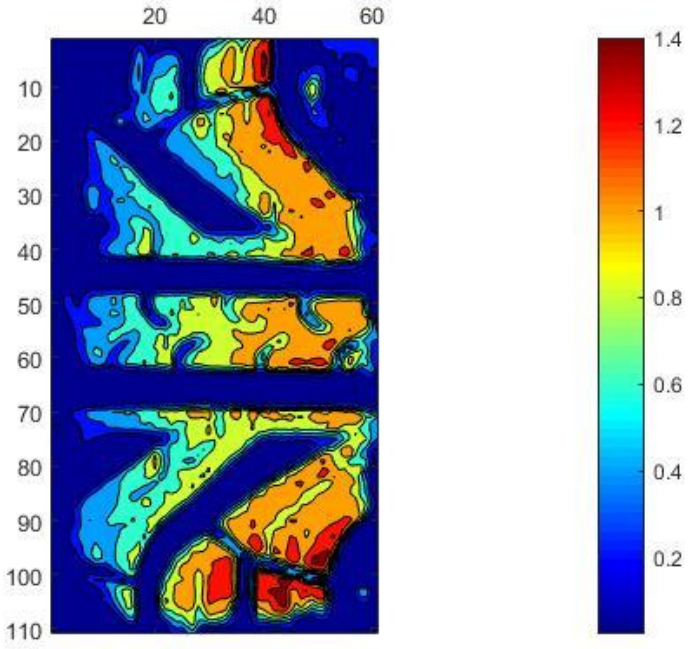

Figure 3.1: Load distribution based on FTIR light intensity at 1 degree of slip angle.

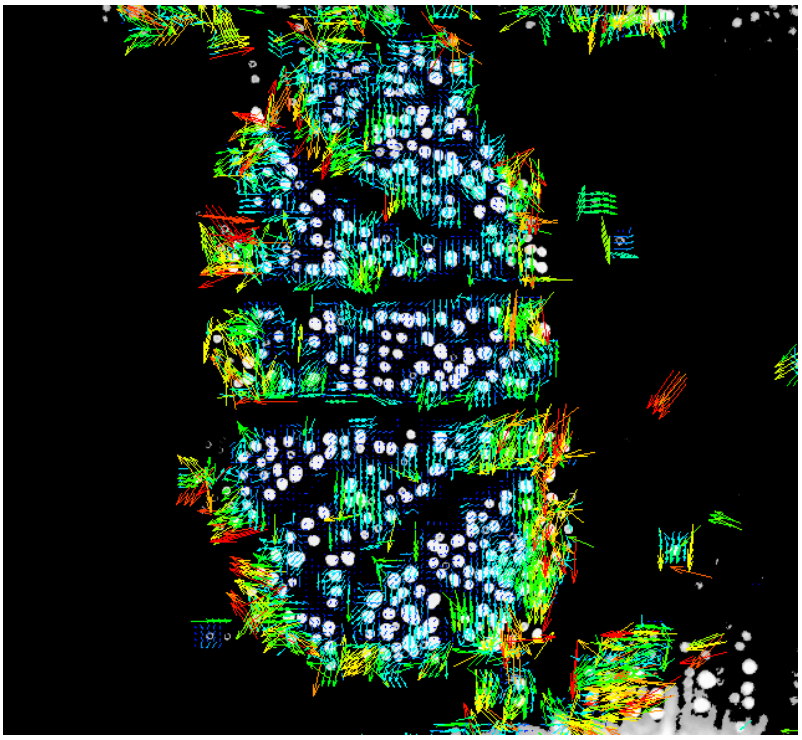

Figure 3.2: Displacement vectors at 1 degree of slip angle.

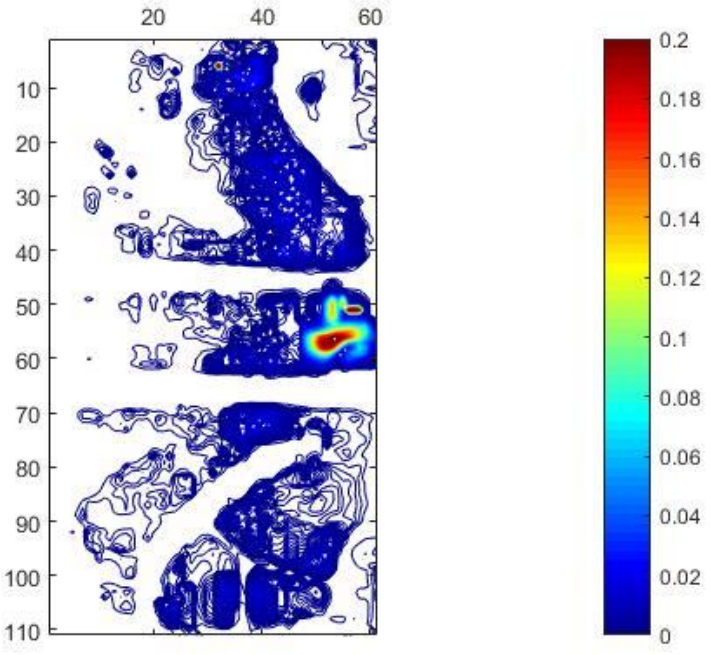

Figure 3.3: Shear energy intensity for 1 degree of slip angle.

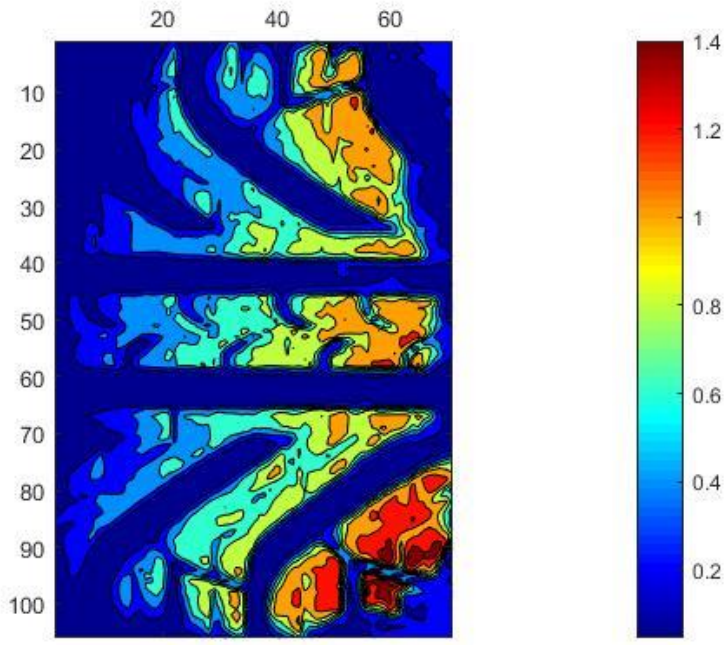

Figure 3.4: Load distribution based on FTIR light intensity at 2 degrees of slip angle.

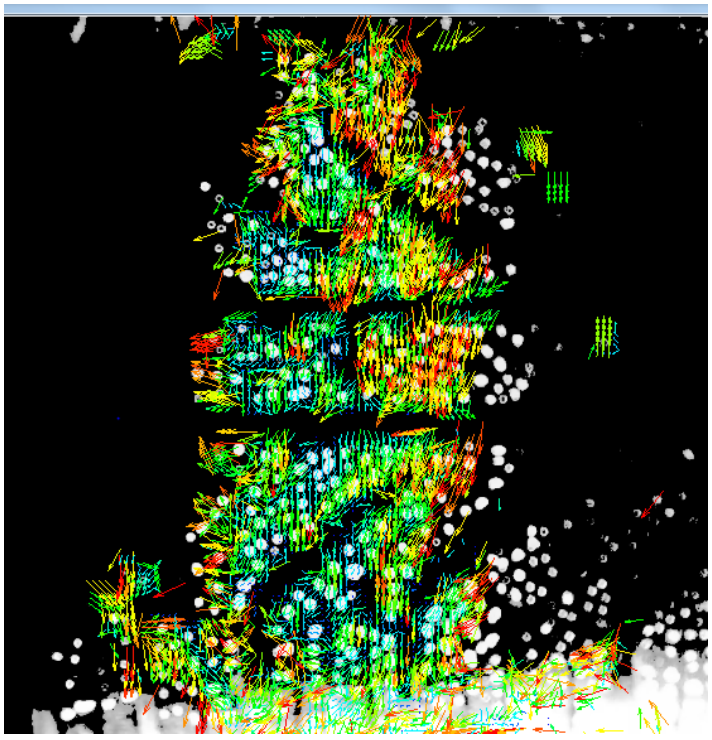

Figure 3.5: Velocity vectors at 2 degrees of slip angle.

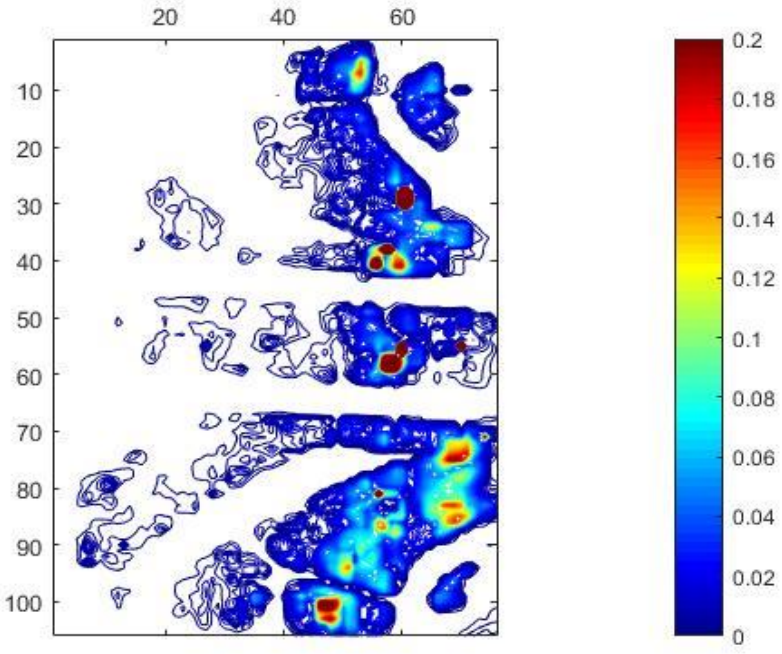

Figure 3.6: Shear energy intensity at 2 degrees of slip angle.

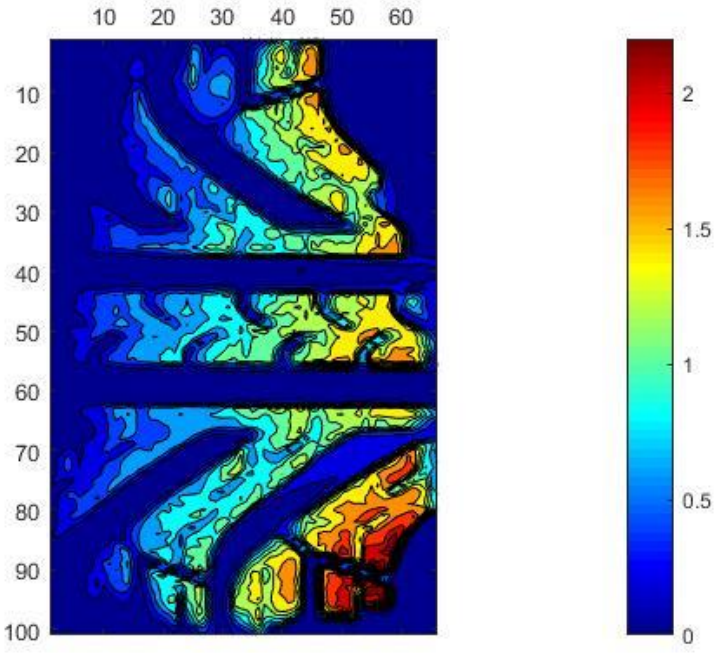

Figure 3.7: Load distribution based on FTIR intensity at 3 degrees of slip angle.

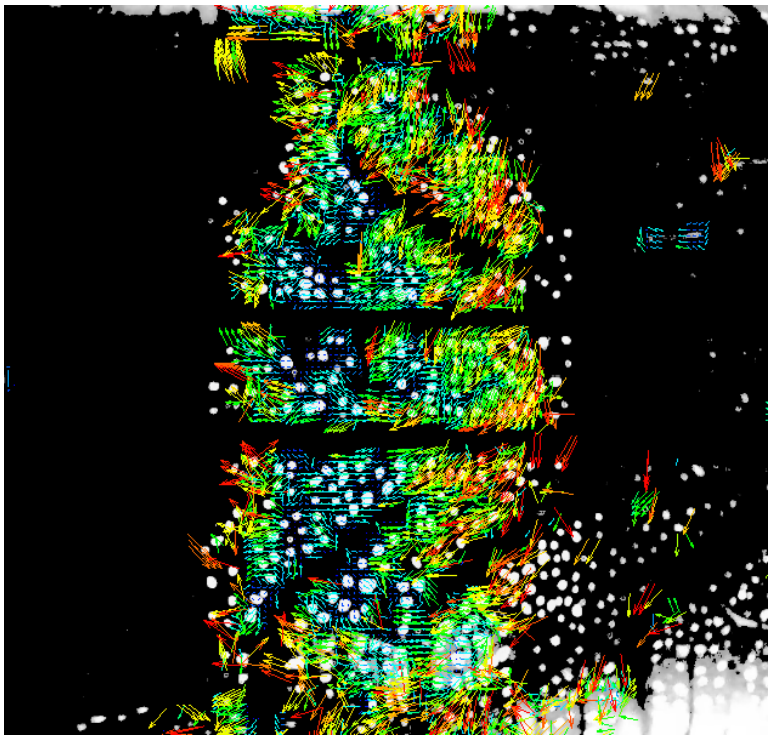

Figure 3.8: Velocity vectors at 3 degrees of slip angle.

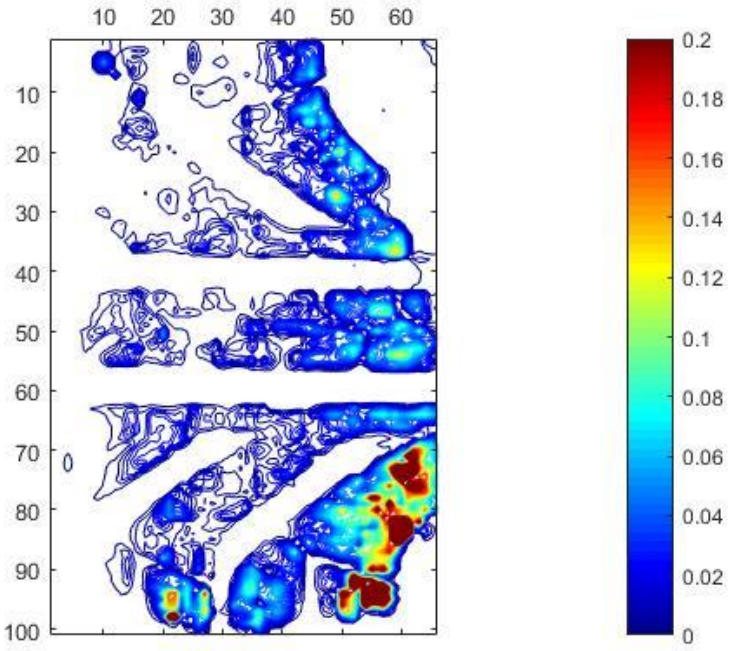

Figure 3.9: Shear energy intensity for 3 degrees of slip angle.

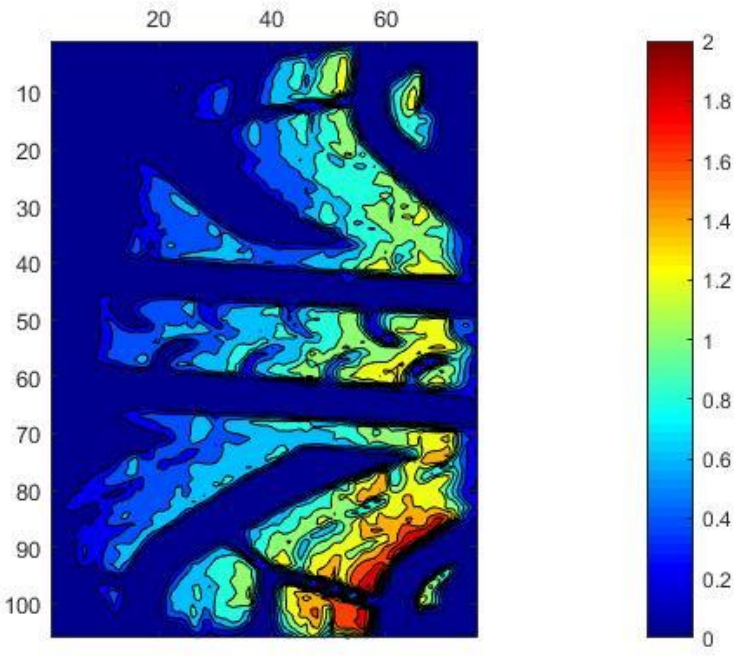

Figure 3.10: Load distribution based on FTIR light intensity for 4 degrees of slip angle.

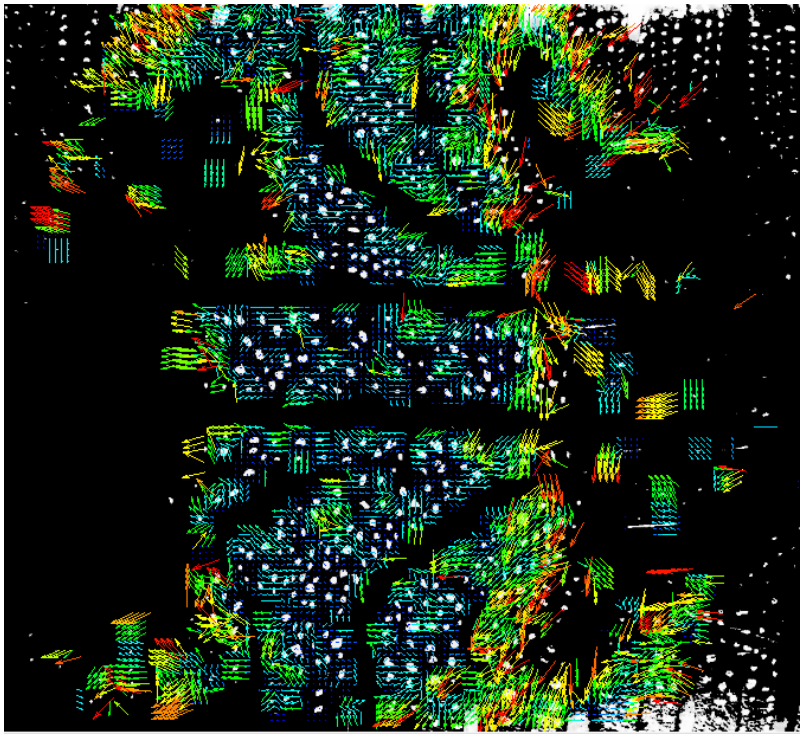

Figure 3.11: Displacement vectors mapped for 4 degrees of slip angle.

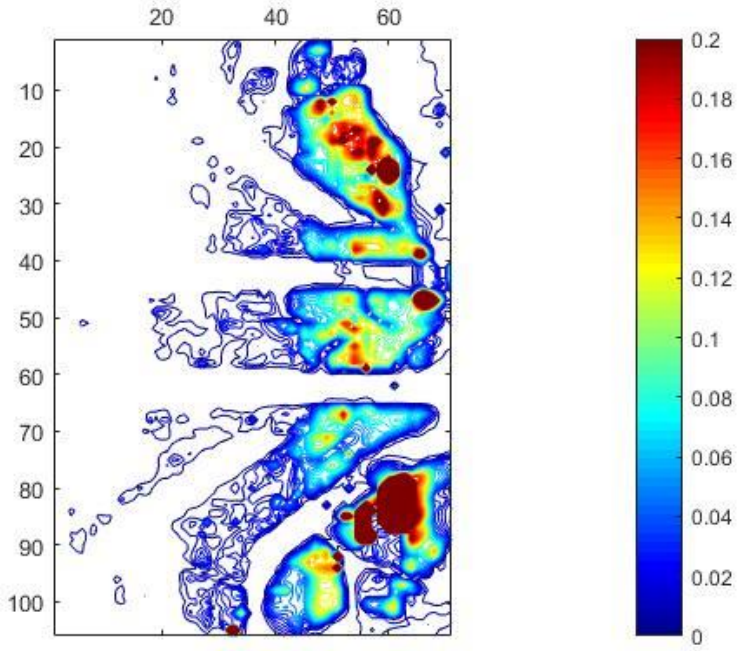

Figure 3.12: Shear energy intensity mapped for 4 degrees of slip angle.

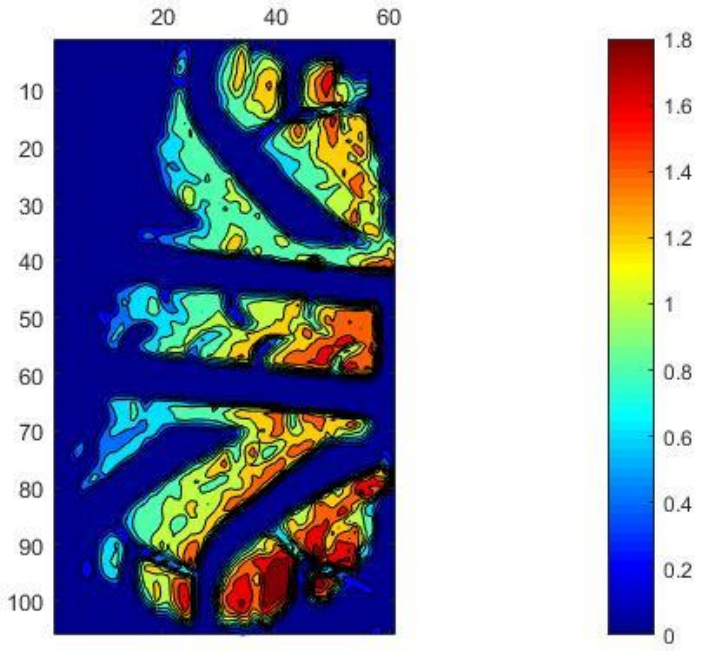

Figure 3.13: Load distribution based on FTIR light intensity at 5 degrees of slip.

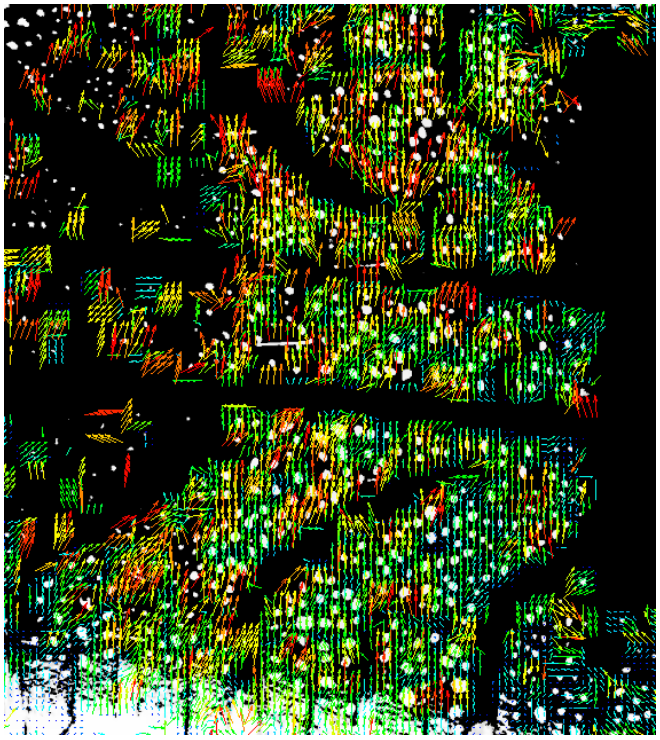

Figure 3.14: Velocity vectors mapped across the contact patch at 5 degrees of slip.

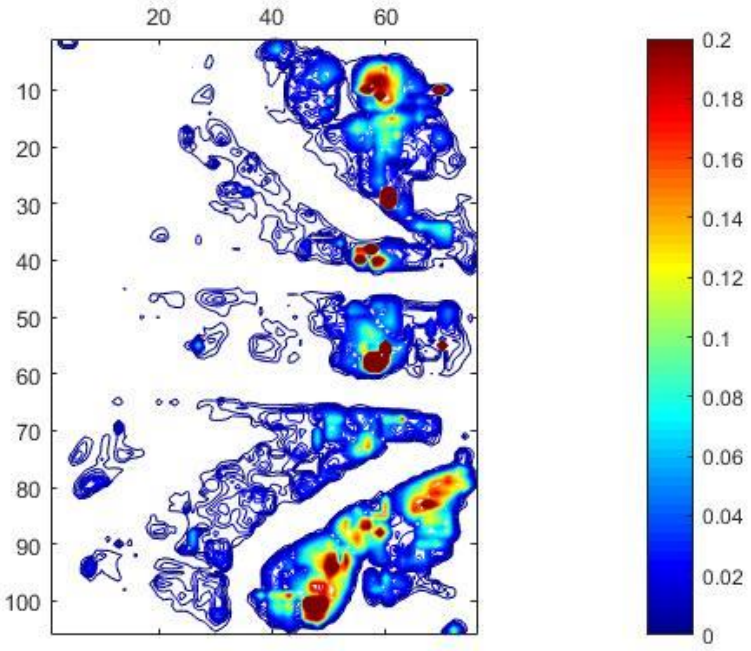

Figure 3.15: Shear energy intensity at 5 degrees of slip.

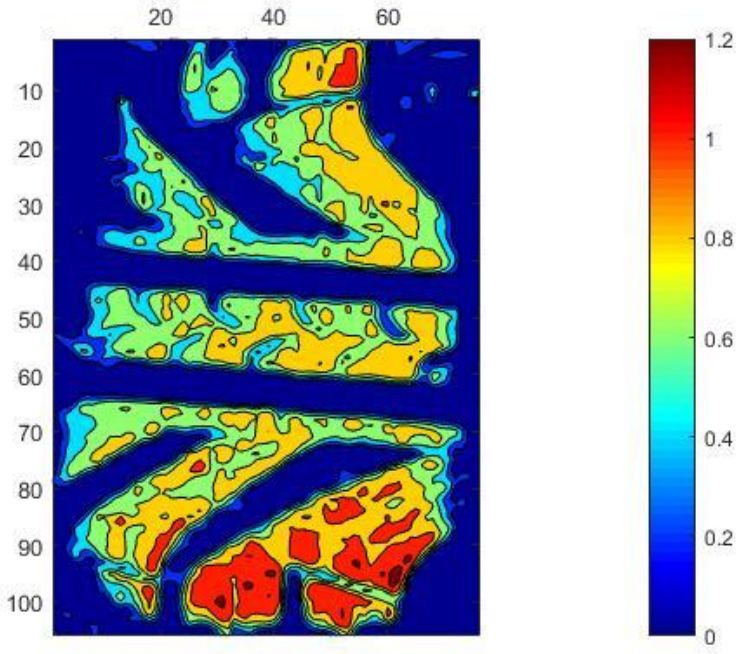

Figure 3.16: Load distribution based on FTIR light intensity at 6 degrees of slip.

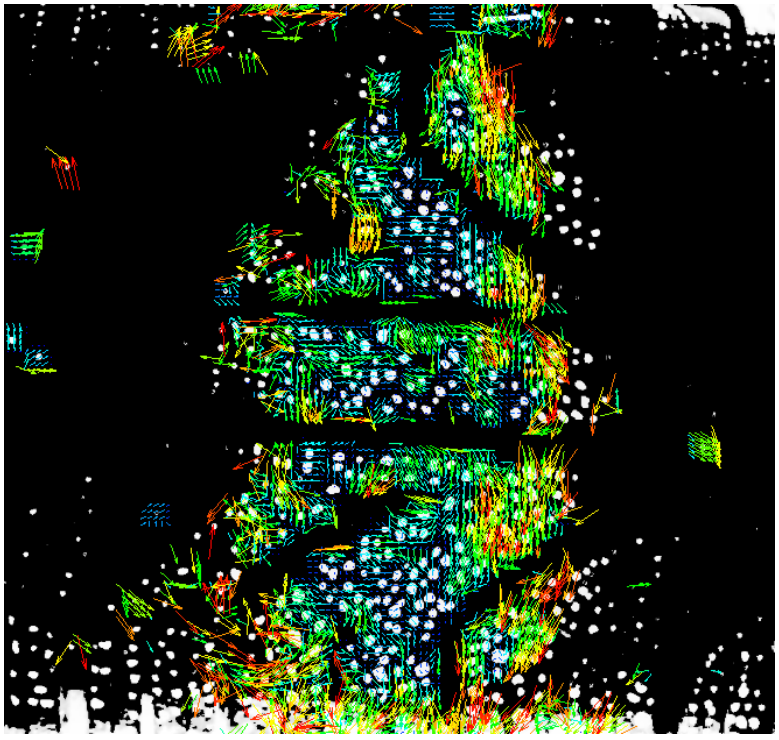

Figure 3.17: Displacement vectors at 6 degrees of slip.

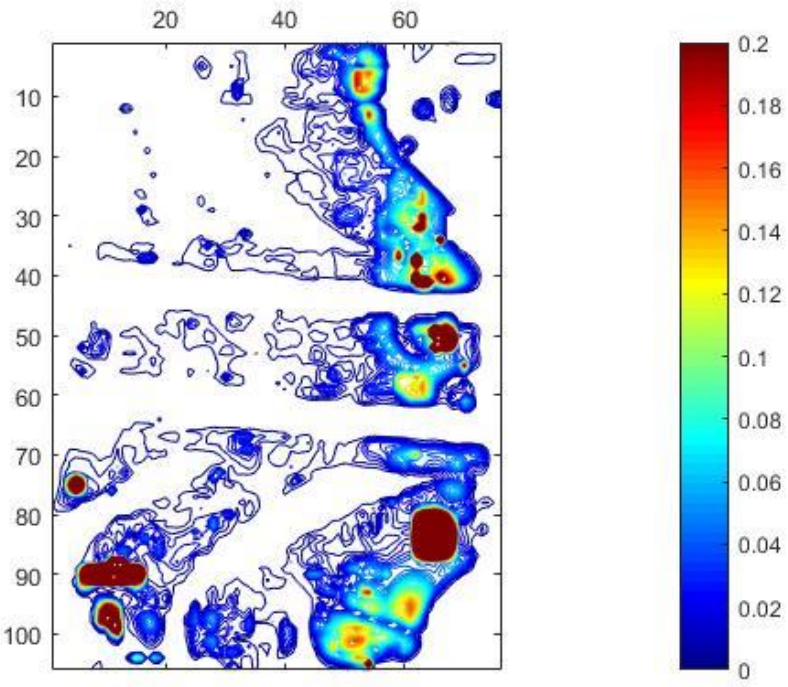

Figure 3.18: Shear energy intensity for 6 degrees of slip.

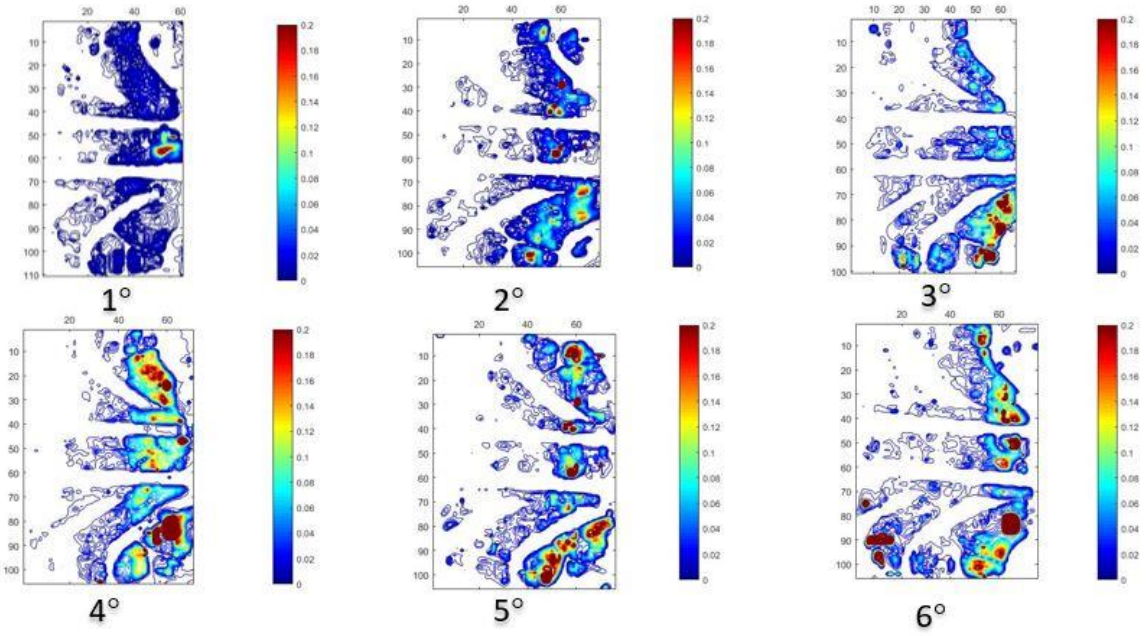

Figure 3.19: Shear Energy Intensity from 1^0 to 6^0 of slip angles.

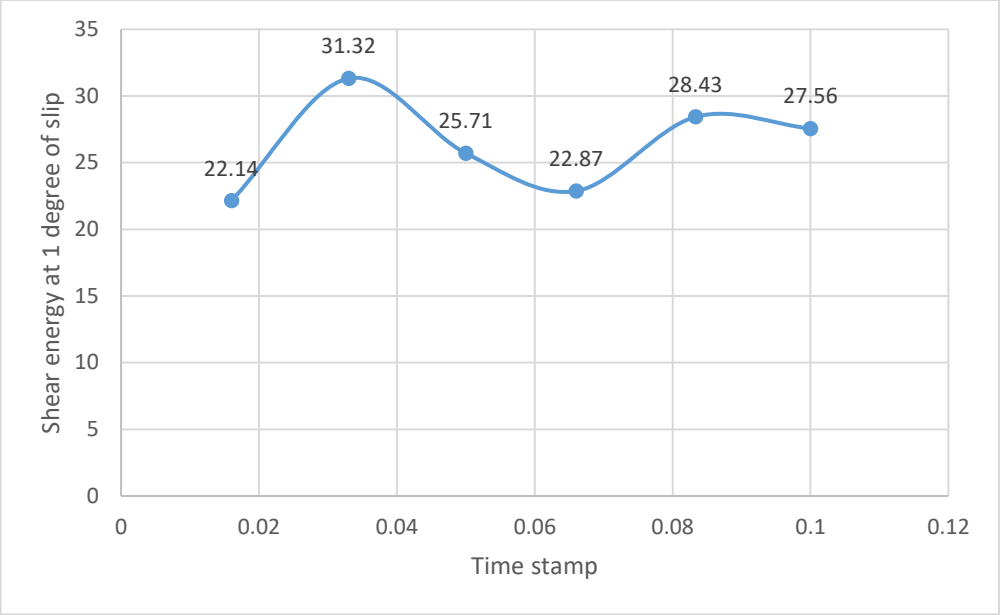

Figure 3.20: Total shear energy for 1 degree of slip angle at different time stamps.

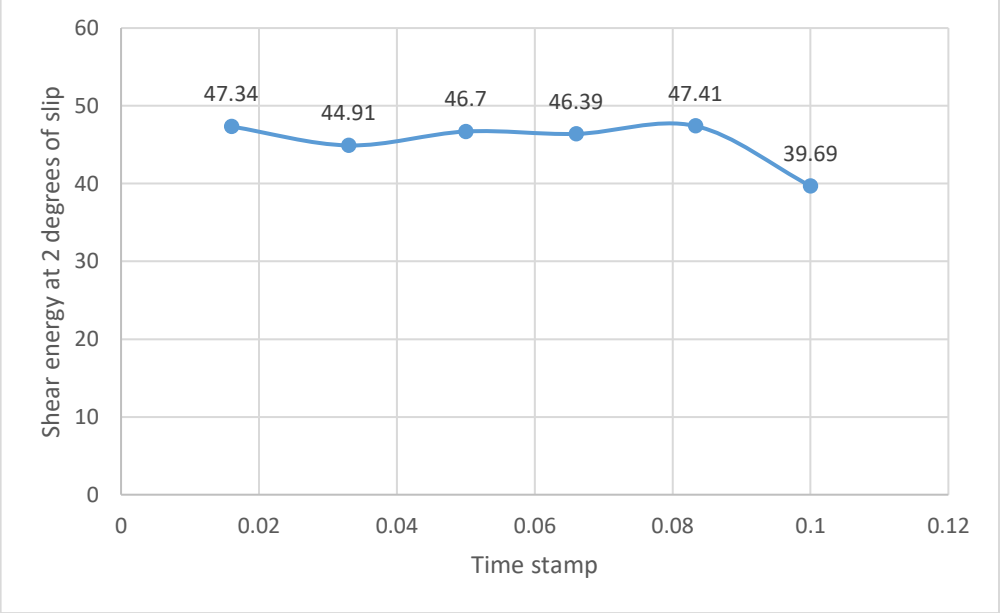

Figure 3.21: Total shear energy for 2 degrees of slip angle at different time stamps.

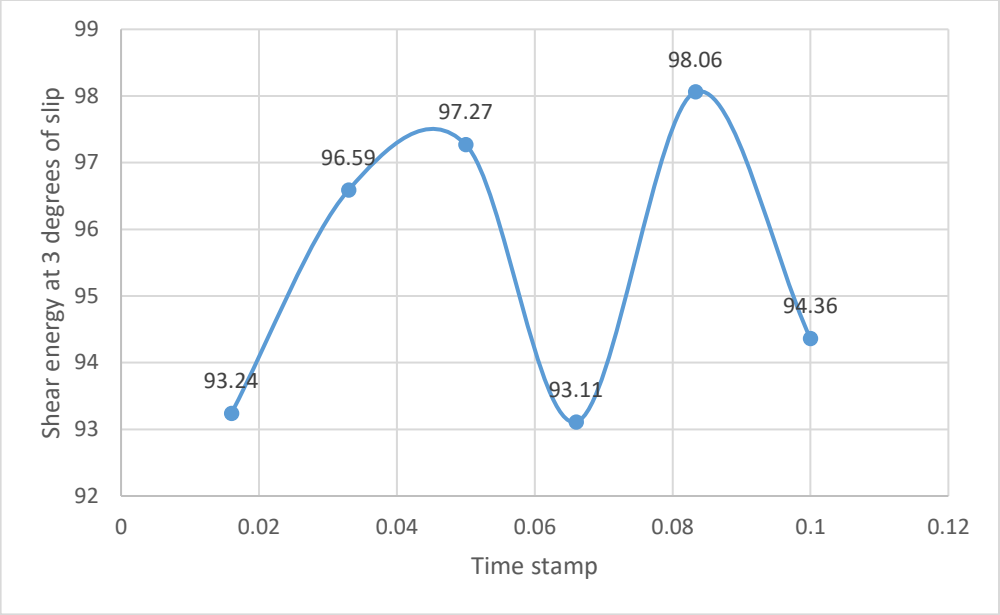

Figure 3.22: Total shear energy for 3 degrees of slip angle at different time stamps.

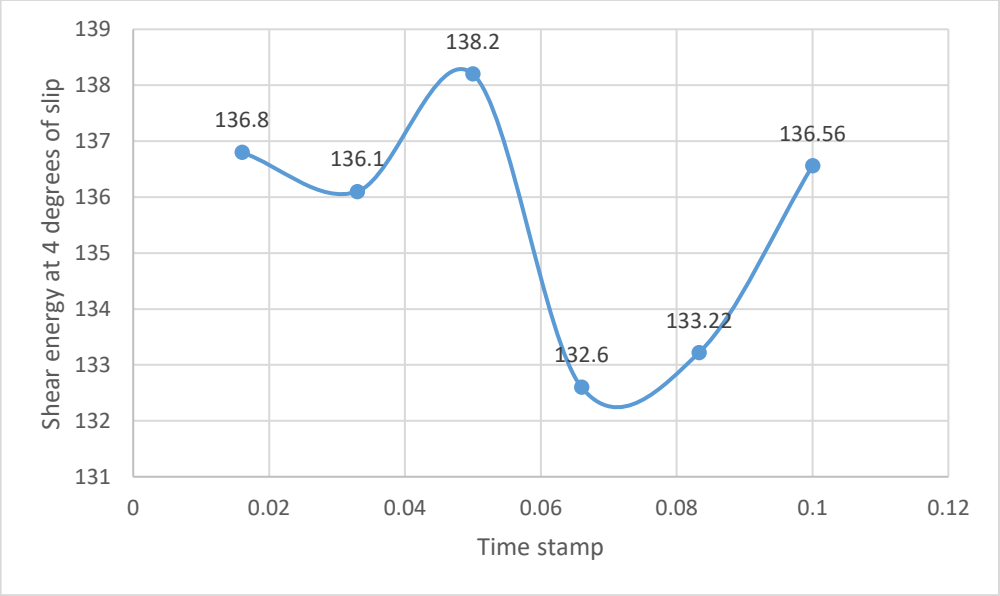

Figure 3.23: Total shear energy for 4 degrees of slip angle at different time stamps.

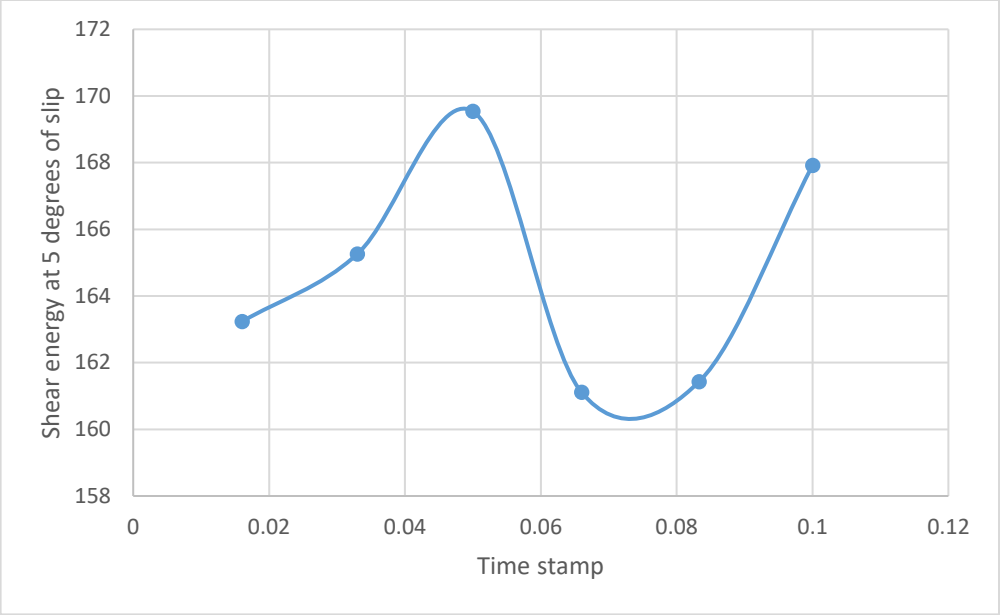

Figure 3.24: Total shear energy for 5 degrees of slip angle at different time stamps.

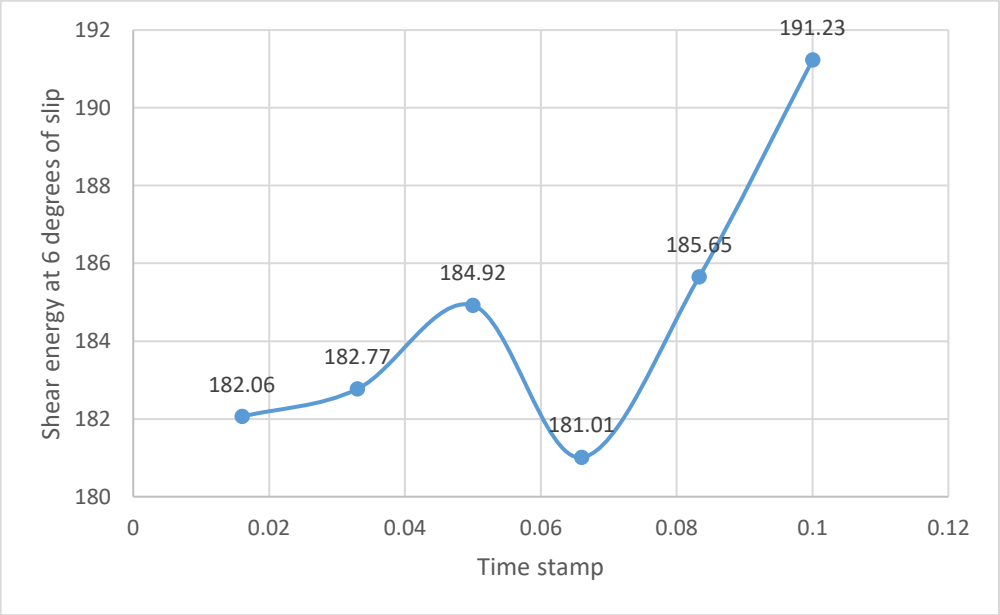

Figure 3.25: Total shear energy for 6 degree of slip angle at different time stamps.

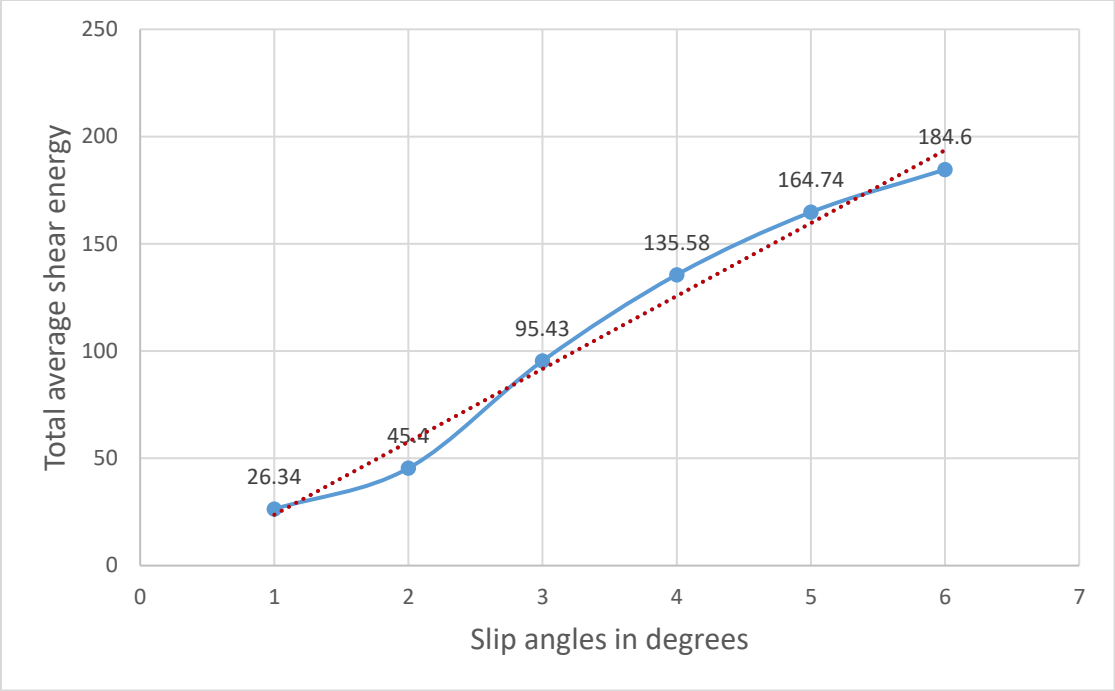

Figure 3.26: Total shear energy across the contact patch for a range of slip angles.

3.2 Conclusion

The shear energy intensity across the contact patch of a rolling tire, mounted on a car with actual suspension settings was successfully mapped for a range of slip angles. As, the shear energy intensity at the contact patch is directly related to tire wear, it can be observed how the tire is going to wear at different slip angles. The results show the shear energy intensity across the contact patch increase with increase in slip angle. This implies that the tire is going to wear more aggressively and have more uneven wear at higher slip angles. From the results, it is seen that the shear energy intensity across the contact patch is more uniformly spread at low slip angles, but as the slip angle increases, the shear energy intensity at the leading edge of the tire is almost close to zero, and the shear energy intensity is very high at the trailing edge of the tire. This is due to the fact that the slip displacements are

maximum at the trailing edge of the tire at higher slip angles. By calculating the total shear energy at various time stamps at each degree of slip angle, the experimental setup was validated, as the total shear energy was found to be within an acceptable range for each degree of slip angle.

3.3 Future work

The future work of this research would include mapping the shear energy intensity across the contact patch for different tire compounds. The shear energy intensity can also be mapped at different pressures for each slip angle to find how the tire is going to wear at different pressures. The amount of tire wear cannot be found by this study as there is no tire abrasion data. By correlating the tire abrasion data with the shear energy intensity, the amount of tire wear can be found.

BIBLIOGRAPHY

[1] C. R. Gentle, "Optical mapping of pressures in tyre contact area," Optics and lasers in engineering, Nottingham, UK, February 1983.

[2] "Contact Patch," [Online]. Available: http://en.wikipedia.org/wiki/contact_patch..

[3] The University of Akron, “The Pneumatic Tire,” G. A.N and W. J.D, Eds., Washington DC: NHTSA, 2005.

[4] Adhikari, B., De, D., and Maiti, S., 2000, Prog. Polym. Sci., 25, 909-948.

[5] Pottinger, M. G., “The Three-Dimentional Contact Patch Stress Field of Solid and Pneumatic Tires”, Tire Science and Technology, TSTCA, Vol. 20, No. 1, 1992.

[6] D. J. Morton, “The Human Foot,” Columbia University Press, New York, 1935.

[7] H. O. Elfman, “A cinematic study of the distribution of pressure in the human foot,” Anatomical Record, 59 (1934) 481-91.

[8] J. Chodera, "Examination Methods of Standing in Man," Vols. 1-3, Fyzilkalni Ustav, Ceskoslovenska Akademie Ved, Prague, 1957.

[9] R. P. Betts and T. Duckworth, “A device for measuring plantar pressures under the sole of the foot,” Engineering in Medicine (I. Mech. E), 7(4) (1978) 223-8.

[10] University of Michigan, “Mechanics of Pneumatic Tires,” Samuel K. Clark, Nat. Bur. Stand. (U.S.), Monogr. 1971.

[11] “PA200 Lite Alignment System,” [Online]. Available: http://www.pro-align.co.uk/proalignproducts/pa200lite.

[12] “Hunter Pro Align Wheel Alignment System,” [Online]. Available: http://www.dpr-motorsport.com/roadandtruck/setups/four wheel alignment.html.

[13] Gillispe, T.D., “Fundamentals of Vehicle Dynamics,” Society of Automotive Engineers Inc., 1992.

[14] Tkacik, P.T., “A Hybrid Model Using The Finite Element Model and Machine vision to Study a Contact Problem,” University of South Carolina, Columbia, SC, 1991.

[15] Gulve, P.M., “Development of a Procedure for Experimental Measurement of Shear Energy Intensity in Tire Contact Patch,” University of North Carolina at Charlotte, Charlotte, NC, 2017.